Formation of Nanostructured Polymer Surfaces from Combined Relaxation and Crystallization

S. Coppée,[†] V. M. Geskin,[‡] R. Lazzaroni,[‡] and P. Damman*,[†]

Laboratoire de Physicochimie des Polymères and Service de Chimie des Matériaux Nouveaux, Université de Mons-Hainaut, 20, Place du Parc, B-7000 Mons, Belgium

Received May 27, 2003
Revised Manuscript Received November 24, 2003

Introduction. The ability to control the topography of polymer surfaces via physical processes is tremendously important and useful in a range of technological applications.[1] Moreover, rubbed polymer films appear to be suitable systems to investigate various physical properties of polymer thin films,[2−10] such as crystallization in confined geometries, chain mobility, dewetting, etc. In fact, many dynamic properties of polymers, like segmental relaxation and chain diffusion, show anomalies for film thicknesses lower than the radius of gyration of the macromolecules (∼50−100 nm).[11] The kinetics of transitions and the morphology of semicrystalline polymers are also modified when confined either in thin layers obtained from block copolymers segregation or in ultrathin films.[12−14]

In this communication, we describe a new method to obtain structured polymer surfaces at different length scales, based on plastic deformations, surface relaxation and crystallization of poly(ethyleneterephthalate), PET, thin films. Several studies showed that a topography induced in polymer films can be fully relaxed above the glass transition.[5−7] However, for "crystallizable" polymers, we can ask the following question: *What is the effect of the "crystallizability" on the surface relaxation*?

Atomic force microscopy (AFM), optical microscopy, and FTIR spectroscopy were used to investigate both relaxation and crystallization processes, which can be observed either subsequently or simultaneously, depending on their kinetics.

Experimental Section. Materials. PET samples were obtained from DuPont (M_w∼ 15−20 kDa, T_g ∼ 80 °C, T_m ∼ 252 °C, and R_g∼ 10 nm). Polyethylene(tere-*ran*-isophthalate) 60/40 copolymer (PET−RAN) was also used to determine the influence of the *crystallizability* on surface relaxation (T_g ∼ 65 °C). The polymer films (thickness ∼ 1 μm) were obtained by casting from dichloroacetic acid solutions onto glass slides and slow evaporation of the solvent at 100 °C overnight (CAST samples). To obtain a reproducible state for the starting sample, the cast films were melted at 272 °C during 60 s and quenched in water. The surface of these initial amorphous films (AMO) is featureless and smooth (root mean square roughness, R_q below 1 nm). Unidirectional rubbing was then performed with a velvet cloth and a homemade machine (pressure, 20 g/cm^2; velocity, 1 cm/s; rubbed distance, 60 cm).[15] These rubbed amorphous samples, called RUB, were submitted to annealing at temperatures slightly above T_g yielding surface-relaxed samples (ANN). Finally, these ANN samples could be heated to 200 °C, to induce cold-crystallization of the polymer (CCR). The sample preparation can thus be summarized as

$$\text{CAST} \rightarrow \text{AMO} \rightarrow \text{RUB} \rightarrow \text{ANN} \rightarrow \text{CCR}$$

Measurements. Thermal relaxation and crystallization were performed with a Mettler FP90 hot stage. Optical observations were carried out with a Leica DMR microscope. The surface morphology of the films was observed with a Nanoscope III A AFM, operated in air, in tapping mode, with commercial 300 kHz tips. The surface roughness was calculated on a lateral scale of 20 μm as the standard deviation of the height for the complete data set (rms roughness). 2D power spectral densities $P_{2i}(s)$ were computed as follows:

$$P_{2i}(s) = \frac{1}{A_i}\left|\int_{A_i} h_i(x, y)\, e^{2\pi j\,(s_x x + s_y y)}\, dx\, dy\right|^2$$

where $h_i(x,y)$ are the height data and A_i is the surface of the image. Circular averaging provided one-dimensional power spectral densities $P_i(s)$:

$$P_i(s) = \frac{1}{2\pi}\int_0^{2\pi} P_{2i}(S, \varphi)\, d\varphi$$

Polarized FTIR spectra were recorded with a Bruker IFS113v spectrometer and an Au grid polarizer. The decoration of polymer surfaces by *p*-nitroaniline (PNA) allowed us to characterize surface chain order since heterogeneous nucleation is particularly sensitive to the substrate molecular order.[16] The crystallization of PNA was performed in a vacuum by direct condensation of the vapor onto the polymer substrates, according to a previously reported method.[17]

Results and Discussion. When rubbing AMO thin films, a shear stress leading to the polymer deformation is applied. From optical microscopy, a birefringence together with a uniform extinction observed for the whole film confirms that the polymer chains orientation is parallel to the rubbing direction. As previously shown, AFM reveals grooves typically 5−10 nm in depth, parallel to the sliding direction (R_q strongly increases, up to a factor of 3, compared to the amorphous films).[15] At this point, we should note that AFM reveals the topography of the films but does not give any indication about local chain orientation. To increase the sensitivity of the FTIR experiment for the surface, we used a decoration method based on vacuum deposition of PNA crystals on the surface. The nucleation of PNA crystals drastically depends on the surface state of the PET at a molecular scale.[18] Only a few PNA crystals nucleate on disordered amorphous surfaces (AMO). In contrast, rubbed PET films are entirely covered by tiny PNA crystals and the overlayer exhibits a strong uniform birefringence. Complete extinction of the layer is observed when the rubbing direction is either parallel or perpendicular to the polarizer. These observations strongly suggest that rubbing induces on the surface a

* To whom correspondence should be addressed. E-mail: pascal.damman@umh.ac.be.
[†] Laboratoire de Physicochimie des Polymères, Université de Mons-Hainaut.
[‡] Service de Chimie des Matériaux Nouveaux, Université de Mons-Hainaut.

10.1021/ma034709c CCC: $27.50
Published on Web 12/18/2003

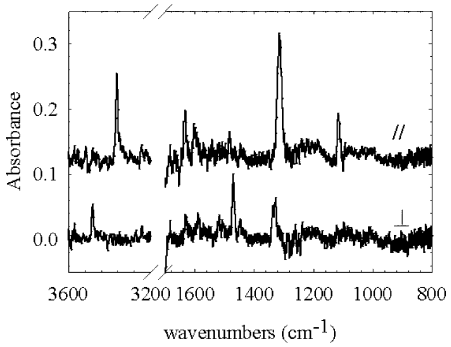

Figure 1. Difference FTIR spectra (obtained by subtraction of PNA-decorated PET RUB − PET RUB spectra). The above (below) spectrum is recorded with a polarized light parallel (perpendicular) to the rubbing direction.

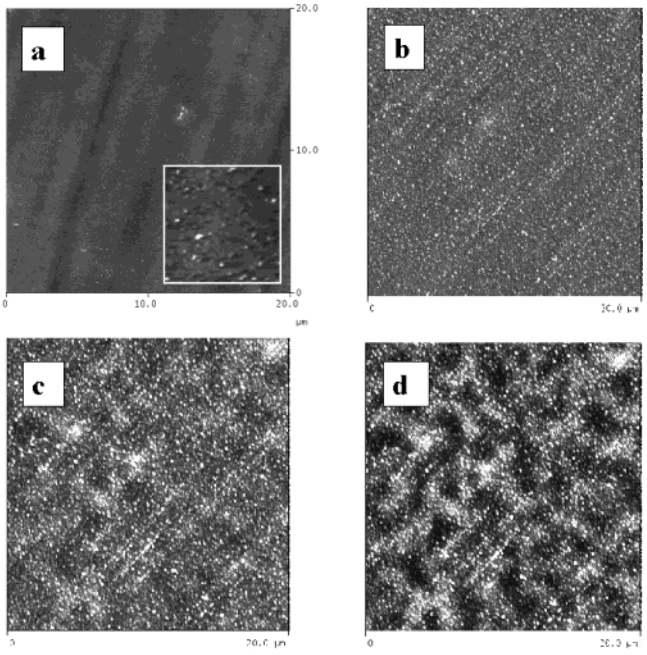

Figure 2. 20 × 20 μm^2 AFM images recorded in situ during the relaxation of a PET rubbed film at 95 °C after (a) 0, (b) 180, (c) 280, and (d) 400 min. The vertical gray scale ranges from 0 to 20 nm. 2 × 2 μm^2 enlarging is inset for 0 min.

strong local chain orientation parallel to the sliding direction. Polarized IR spectra of PNA/PET layers confirm these observations (Figure 1). The observed dichroism indicates a *quasi perfect orientation* of all the crystals with respect to the sliding direction (see for instance: $\nu^s_{NH_2}$ at 3354 cm^{-1} and $\nu^s_{NO_2}$ at 1300 cm^{-1}).[19]

Relaxation. Previous works showed that a topography induced in amorphous polymer surfaces vanishes upon annealing.[5−7] As previously shown, the initial birefringence observed for rubbed PET and PET−RAN films vanishes during the relaxation at T_g.[15] In the same way, the AFM images show a drastic decrease of the surface roughness, its final value being only ∼1 nm. Except for the deepest ones, all the grooves disappear upon annealing. However, for PET films, a closer examination of the AFM images shows that the surface is not totally smooth. Small bright domains are distributed rather homogeneously on the film surface (Figure 2a). Their diameter and height are ∼100 nm and ∼5 nm, respectively. These domains account for the residual roughness, which is significantly higher (R_q = 1.4 nm) than that of the initial amorphous films (R_q = 0.6 nm). The surface decoration can be used to test the

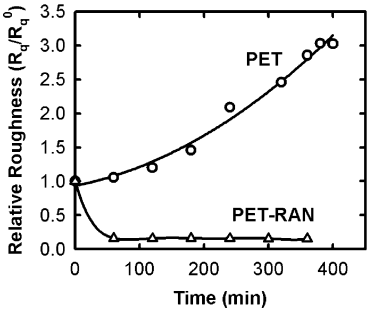

Figure 3. Evolution of the relative roughness computed from AFM images (R_q/R_q^0) during the relaxation of rubbed PET and PET−RAN films at T_g + 15 °C. The initial rms roughnesses were 3.0 and 5.0 nm for PET and PET−RAN, respectively.

local surface ordering. From optical micrography of PNA vapor-decorated ANN films, we found that the surface ordering induced by rubbing is maintained during and after the surface relaxation. These observations strongly suggest that the small bright domains appearing on the relaxed surface (Figure 2) are probably related to crystalline aggregates. Since they preserve the unidirectional orientation induced by rubbing, we can consider that these aggregates are formed during the relaxation process of the stressed material. We note however that this morphology is not observed for *uncrystallizable* polymers (PET−RAN).

To determine the origin of this peculiar morphology, the relaxation process was followed in situ at $T \sim T_g$ + 15 °C for PET and PET−RAN rubbed films with the temperature-controlled AFM. During the relaxation of PET−RAN (*uncrystallizable*) at 85 °C, we observed a fast decrease of the surface roughness with time, down to a minimum value of 0.7 nm (Figure 3). The plots of the power spectral density ($P(s)$) vs the reciprocal distance (s) were computed from the AFM images (Figure 4a). In agreement with previous work about the capillary waves spectra of amorphous polymer surfaces, we found a power law evolution for the PSD. In this frequency range, $P(s)$ decreases as s^{-2}.[20]

In contrast with PET−RAN, the relaxation of PET films (*crystallizable*) at 95 °C shows a continuous increase of the surface roughness with time; R_q can reach values as high as 10 nm (Figure 3). This increase in surface roughness can be related to the formation of corrugations on the polymer surface (see Figure 2, parts b−d). As shown in the AFM images and in the power spectral density (PSD) spectra (Figure 4b), a hierarchical structure with two well-defined features is observed. We note that the first maximum in the PSD spectra, characteristic of the smallest corrugations, increases with time (from 250 to 400 nm) while the largest surface ripples have a rather constant wavelength (∼3 μm).

However, we believe that all the observed corrugations must be related to the crystallization of PET, although the origin of the smallest and largest waves is different. The lateral extent of the smallest corrugations, ∼200 nm, is very large as compared to the typical size of polymer crystals (i.e., parallel to the chain direction, the crystals usually extend only a few tens of nanometers). Therefore, we propose that the corrugations are directly related to the surface stress associated with the crystallization. Indeed, the surface must shrink to accommodate the increase in density observed during the crystallization (i.e., $\rho_c > \rho_a$).

As for the largest corrugations (∼3 μm), we propose that they are formed via an amplification of surface

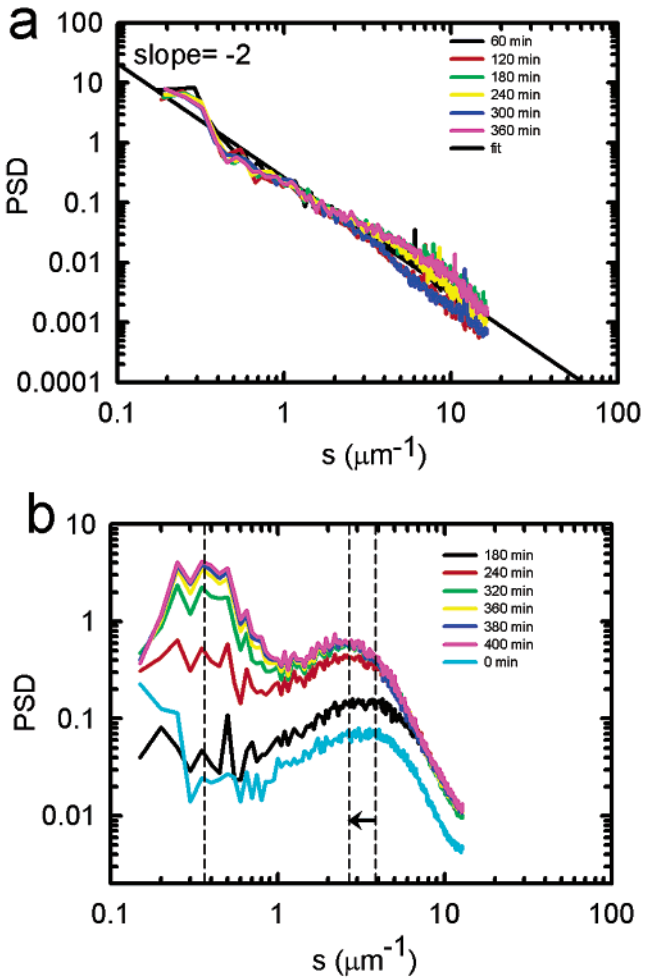

Figure 4. Log−log plots of the power spectral density, $P(s)$, vs the reciprocal distance, s, as computed from the AFM images recorded during the relaxation of (a) PET−RAN film at 85 °C and (b)PET film at 95 °C.

waves due to the density fluctuations associated with crystallization. Indeed, the observed morphology is reminiscent of a spinodal mechanism. Recently, Sharma et al. reported that a *density variation induced instability* of film surfaces could mimic a spinodal morphology.[21] From a theoretical approach, they demonstrate that an increase(decrease) in density with the film thickness stabilizes (destabilizes) the film surface. At first sight, this seems to be in contradistinction to our observations (due to the crystallization, $\rho_{surf} > \rho_{bulk}$). However, we can reconcile these results by considering that the crystallization of the film destabilizes the surface, provided that this crystallization is confined to the outer surface of the film (this is really achieved by the rubbing process).[15] In this case, the crystallized outer surface directly exerts a constraint on the amorphous inner region. This constraint destabilizes the polymer surface that ripples to release the surface stress. The relation between the periodicity of the corrugations and the crystallization process is under investigation.

Crystallization. As shown here above, the crystallization appears to begin well below the usual crystallization domain ($T_c \sim 142$ °C). The stretching of the crystallization domain toward lower temperatures could be due to the chain alignment during the film rubbing which makes the formation of crystalline nuclei easier. The comparison of optical micrographs of rubbed crystallized films (CCR) and unrubbed crystallized samples shows contrasting morphologies. The unrubbed film presents the spherulitical morphology typical of semicrystalline polymers. In contrast, the rubbed CCR film exhibits a strong birefringence and a complete extinction when the sliding direction is either parallel or perpendicular to the polarizers. These observations are consistent with a uniform orientation of the chains axis parallel to the rubbing direction. The rate of crystal formation is drastically enhanced in deformed polymer thin films, due to the metastable character of the preoriented layer. Such mode of growth yields polycrystalline films with a uniform orientation.

The IR spectra of the PET CCR film recorded with a beam polarized parallel and perpendicular to the rubbing direction confirm these observations. The surface orientation propagates to the whole film as suggested by the observed dichroism. We can therefore consider that the crystalline aggregates, which appear on the surface vicinity during relaxation, act as nuclei that propagate the orientation to the film areas too deep to be affected by rubbing. This kind of crystallization can be related to epitaxial growth, in which an organized surface is used as a template to initiate a bulk crystallization.

Conclusions. Our observations confirm that the dissipation of mechanical energy upon rubbing induces plastic deformations, appearing as parallel grooves of varying depth, and alignment of the chains along the rubbing direction. During the relaxation of the rubbed surfaces, the formation of a hierarchical surface structure with two characteristic wavelengths (∼200 nm and ∼3 μm) is observed. We suggest that the small corrugations are directly related to the surface stress associated with the crystallization (the polymer surface has to shrink to accommodate the increase in density associated with the crystallization). The largest corrugations arise from the confinement of crystallization to the outer surface and from the stress exerted by the crystallized surfaces to the amorphous region.

Our results thus show that a combination of different physical processes, such as plastic deformation, surface relaxation, and crystallization, is actually a suitable method to generate polymer surfaces with a well-defined topography.

Acknowledgment. The authors acknowledge D. Villers, A. Jonas, P. Viville, and G. Reiter for stimulating discussions. S.C. thanks the "Fonds pour la Formation à la Recherche dans l'Industrie et dans l'Agriculture" (FRIA, Brussels) for financial support. This work was supported by the Belgian National Fund for Scientific Research (FNRS), by the Belgian Federal Government "Service des Affaires Scientifiques, Techniques et Culturelles (SSTC)" in the framework of the "Pôle d'Attraction Interuniversitaire en Chimie Supramoléculaire et Catalyse Supramoléculaire (PAI V/3)", and by the "Région Wallonne" and the European Commission, in the framework of Phasing-out Hainaut. P. Damman and R. Lazzaroni are Research Associate and Research Director of the FNRS, respectively.

References and Notes

(1) Xia, Y.; Qin, D.; Yin, Y. *Curr. Opin. Colloid Interface Sci.* **2001**, *6*, 54.
(2) Van Aerle, N. A. J. M.; Barmentlo, M.; Hollering, R. W. J. *J. Appl. Phys.* **1993**, *74*, 3111.
(3) Toney, M. F.; Russell, T. P.; Logan, J. A.; Kikushi, H.; Sands, J. M.; Kumar, S. K. *Nature (London)* **1995**, *374*, 709.

(4) Hähner, G.; Spencer, N. *Phys. Today* **1998**, *09*, 22.
(5) Liu, Y.; Russell, T. P.; Samant, M. G.; Stöhr, J.; Brown, H. R.; Cossy-Favre, A.; Diaz, J. *Macromolecules* **1997**, *30*, 7768.
(6) Schwab, A. D.; Agra, D. M. G.; Kim, J. H.; Kumar, S.; Dhinojwala, A. *Macromolecules* **2000**, *33*, 4903.
(7) Pu, Y.; White, H.; Rafailovich, M. H.; Sokolov, J.; Schwarz, S. A.; Dhinojwala, A.; Agra, D. M. G.; Kumar, S. *Macromolecules* **2001**, *34*, 4972.
(8) Du, B.; Xie, F.; Wang, Y.; Yang, Z.; Tsui, O. K. C. *Langmuir* **2002**, *18*, 8510.
(9) Tsang, O. C.; Xie, F.; Tsui, O. K. C.; Yang, Z.; Zhang, J.; Shen, D.; Yang, X. *J. Polym. Sci., Polym. Phys.* **2001**, *39*, 2906.
(10) Tsang, O. C.; Tsui, O. K. C.; Yang, Z. *Phys. Rev. E* **2001**, *63*, 061603.
(11) Jones, R. A. L. *Curr. Opin. Colloid Interface Sci.* **1999**, *4*, 153.
(12) Forrest, J. A.; Dalnoki-Veress, K. *Adv. Colloid Interface Sci.* **2001**, *94*, 167.
(13) Hamley, I. W. *The Physics of Block Copolymers*; Oxford University Press: Oxford, England, 1998.
(14) Reiter, G.; Sommer, J.-U. *Phys. Rev. Lett.* **1998**, *80*, 3771.
(15) Damman, P.; Zolotukhin, M. G.; Villers, D.; Geskin, V. M.; Lazzaroni, R. *Macromolecules* **2002**, *35*, 2.
(16) Wittmann, J.-C.; Lotz, B. *Electron Crystallography of Organic Molecules*; Fryer, J. R., Dorset, D. L., Eds.; Kluwer Academic Publishers: Dordrecht, The Netherlands, 1990; p 241.
(17) Vallée, R.; Damman, P.; Dosière, M.; Toussaere, E.; Zyss, J. *J. Am. Chem. Soc.* **2000**, *122*, 6701.
(18) Damman, P.; Coppée, S.; Geskin, V. M.; Lazzaroni, R. *J. Am. Chem. Soc.* **2002**, *124*, 15166.
(19) Damman, P.; Dosière, M.; Brunel, M.; Wittmann, J.-C. *J. Am. Chem. Soc.* **1997**, *119*, 4633.
(20) Bollinne, C.; Cuenot, S.; Nysten, B.; Jonas, A. M. *Eur. Phys. J. E*, in press (special issue on Unstable Thin Films).
(21) Sharma, A.; Mittal, J. *Phys. Rev. Lett.* **2002**, *89*, 186101.

MA034709C